River Flow 2010 - Dittrich, Koll, Aberle & Geisenhainer (eds) - © 2010 Bundesanstalt für Wasserbau ISBN 978-3-939230-00-7

Aspects of turbulence and fine sediment resuspension in accelerating and decelerating open-channel flow

F. Bagherimiyab & U. Lemmin
Ecole Polytechnique Fédérale de Lausanne (EPFL), ENAC, Station 18, CH-1015 Lausanne, Switzerland

ABSTRACT: Hydrodynamic aspects of unsteady (accelerating and decelerating) depth-varying open-channel flow over a gravel bed were investigated. Using acoustic Doppler and imaging methods, quasi-instantaneous profiles of velocity and sediment concentration were taken simultaneously and co-located with spatial and temporal resolution of turbulence scales. A high-speed camera allowed for fine sediment resuspension visualization. During the unsteady flow without fine sediment, the profiles of mean longitudinal velocity have a logarithmic shape in the inner layer. Bottom shear velocity at the beginning and at the end of the accelerating and decelerating unsteady flow ranges is similar and it increased more rapidly during the initial phase of the accelerating flow range than the mean velocity. This indicates that an internal adjustment takes place which may affect the turbulence structure responsible for particle resuspension. However, bottom shear velocity decreased linearly in the decelerating flow range. Fine sediment was resuspended in bursts and rapidly created nearly stationary ripples during the final phase of the accelerating flow range. Vortices shedding from the ripple crests produced most of the sediment resuspension in events, making resuspension intermittent. Hydraulic parameters, such as water depth, mean velocity time development and profile form were not affected by the presence of fine sediment particles.

Keywords: *Accelerating flow, Decelerating flow, Resuspension, Bottom shear velocity, ADVP*

1 INTRODUCTION

Studies of turbulent unsteady flow in open channels indicate that insight into the structure of turbulence is important in order to advance the understanding of sediment flux development because of its impact on physical, chemical, biological and ecological processes in the water column. Hayashi et al. (1988) using a hot-film anemometer, suggested that turbulence is stronger in the rising stage than in the falling stage. Nezu & Nakagawa (1993) found that the log law is still valid in unsteady open-channel flows. Nezu & Nakagawa (1993) estimated the friction velocity u_* and the wall shear stress ρu_*^2 as a function of time. Nezu et al. (1997) verified that the values of wall shear stress estimated from the aforementioned log law coincide reasonably well with those evaluated from the momentum equation.

In oscillatory closed-channel flows, Jensen & Sumer (1989) and Akhavan et al. (1991) observed that the mean velocity obeyed the log law distribution, except at the very early stages of the acceleration phase and the late stages of the deceleration stage.

By measuring turbulence structure over a smooth wall in unsteady depth-varying open channel flows, Nezu et al. (1997) established that in the rising stage, the wall shear stress attains its maximum ahead of the flow depth. They also detected hysteresis loop properties of velocity and turbulence profiles in unsteady open-channel flows. Afzalimehr & Anctil (2000) studied spatially accelerating shear velocity in gravel-bed channels. They showed that the logarithmic law is valid for gravel-bed channels, as long as it is applied to the inner layer of the flow ($y/h \leq 0.2$).

Suspension of sediment particles occurs when the local bottom shear stress exceeds the critical value (Shields 1936). Initiation of sediment motion which occurs due to unsteady turbulent water flows is an important aspect of river and coastal engineering. Under steady flow conditions, suspension may be caused by secondary currents (Nezu & Nakagawa 1993) or coherent structures (Nezu & Nakagawa 1993, Cellino & Lemmin 2004, Nezu 2005). Sediment transport studies in

unsteady flow (Sutter et al. 2001) indicate a hysteresis loop in sediment concentration, similar to that observed in turbulence intensities by Nezu et al. (1997).

All these studies demonstrate that determining the structure of turbulence in unsteady flow is important in order to advance the understanding of sediment flux development.

We will first briefly describe the instruments used and the experimental procedure. The results will be discussed thereafter.

2 EXPERIMENTAL SET-UP

The measurements were carried out in a glass-walled open-channel which is 17 m long and has a rectangular cross section 0.6 m wide and 0.8 m deep. The bottom is covered with a 0.1 m thick gravel layer (size range 3 to 8 mm; D_{50} = 5.5 mm). The channel is operated in closed circuit mode. Pump discharge is modified by changing the rotational speed of the pump by computer. A shallow weir at the end of the channel controls the water level. The water level in the channel is measured with four ultrasonic limnimeters spaced along the channel. The bed of the channel is horizontal.

2.1 *Acoustic Doppler particle flux profiling in unsteady flow*

Acoustic Backscattering Systems (ABS) allow capturing the Doppler phase angle and the intensity of the backscattered signal. The Doppler phase angle has been used in Acoustic Doppler Velocity Profilers (ADVP; Lhermitte & Lemmin 1994). The backscattered intensity can be inverted into particle concentration after calibration (Thorne & Hanes 2002). It is important to provide proper attenuation compensation either by hardware (Shen & Lemmin 1996) or by software (Hurther et al. 2007; Bricault 2006) methods. By integrating either method into the existing ADVP, a particle flux profiler was developed at our laboratory that determines the 3D velocity field and the suspended particle concentration field co-located in the same scattering volumes of the profile, even at high particle concentrations.

The emitter and the receivers of the ADVP are placed in a water-filled housing which is installed above the water surface, and which slightly touches the flow. The ADVP has to follow the surface in the depth-varying region of the hydrograph (Figure 1). This is done by a computer-controlled system. ADVP profiling was carried out on the centerline of the channel about 15 m from the entrance where turbulence is well developed. A 1 cm thick layer of the water column near the water surface was omitted from the analysis, because the flow in this layer is slightly perturbed by the instrument.

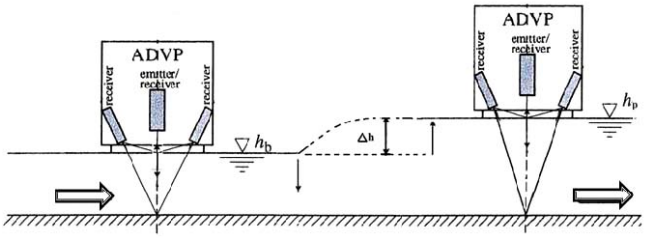

Figure 1. Schematics of the ADVP instrument in unsteady flow

2.2 *Experimental procedure*

The hydrograph for the experiment consists of 5 parts. The flow is first maintained at the base discharge with $h = h_b$ for 90 s, followed by the rising stage of the unsteady flow (accelerating) where the discharge is linearly increased by computer control over a period of 30 s. Then the peak flow is steady at $h = h_p$ for 60 s (Figure 1). Thereafter discharge is linearly decreased during the falling stage of the unsteady flow (decelerating) over a period of 30 s to the initial base discharge. The pump discharge, the ADVP, and limnimeter data are simultaneously recorded during the hydrograph. In order to obtain reliable data during the unsteady phase, the same experiment is repeated. Since the whole experiment is computer controlled, the deviations between individual experimental runs were less than 3%.

Table 1 gives the range of the discharge, water depth, and Reynolds number at the base and peak flow of the hydrograph investigated here. No sediment transport occurred under the initial conditions.

Table 1. Range of variations of discharge, water depth and Reynolds number during unsteady flow

		Base	Peak
Pump discharge Q	(l sec^{-1})	9.3	32.7
Water depth	(cm)	12	17
Reynolds Number		1.1×10^4	4.5×10^4

In order to investigate the resuspension of fine sediment particles, a layer of sand with D_{50} = 0.16 mm was spread on top of the coarse bed on a surface area of the channel extending about 1 m upstream from the location of the ADVP. For the present study, this layer was thick enough to fully cover the coarse bed by about 4 mm and thus smoothed out bed roughness. The acoustic measurements were complemented by simultaneously taking high-speed videos in the center of the channel, just upstream of the ADVP location. Only a narrow slot (40 cm long and about 1 cm in the

transversal depth) of the flow in the center of the channel was illuminated by a light sheet.

Two sets of experiments were carried out. In the first set, no fine sediment was placed on the rough bed. During these experiments, hydrogen bubbles were generated as flow tracers for the ADVP measurements (Blanckaert & Lemmin 2006). In the second set of experiments, fine sediment was added to the bed as described above and no hydrogen bubbles were produced. In these experiments, only sediment particles served as tracers for the ADVP measurements. Thus, only the flow field which activates sediment resuspension is documented in these experiments. All ADVP data were de-aliased (Franca & Lemmin 2006) and de-noised (Blanckaert & Lemmin 2006) to improve data quality.

Figure 2 shows the variation of water level near the ADVP for the 5 parts of the hydrograph which is representative for all experiments discussed here. Even though the pump discharge is varied linearly in the course of the accelerating and decelerating stages, water depth changes non-linearly throughout these periods. When the pump discharge was kept constant at peak flow, water depth still slowly increased and did not reach steady state. The discrepancy between the variation of the pump discharge and the observed water level over time indicates that along the channel, flow adjustment over the rough bed takes place.

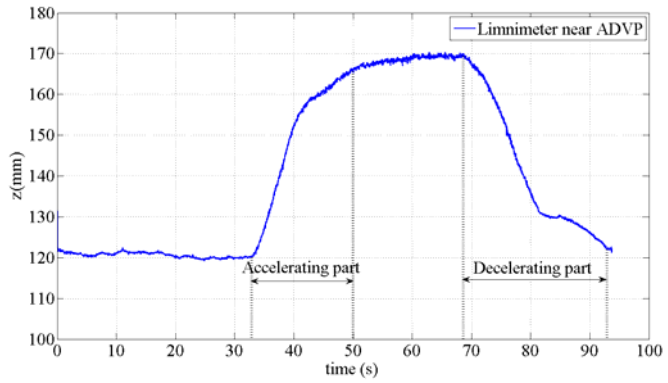

Figure 2. Variation of water level recorded near the ADVP

3 RESULTS

3.1 *Velocity measurements*

In order to compare the results for the unsteady accelerating and decelerating flow ranges, time development curves of the parameters in the two flow ranges were plotted in the same figure. Therefore, in the following figures, curves for the decelerating flow are shown reversed in time.

Since logarithmic profiles were expected in the inner layer (Bagherimiyab & Lemmin 2009; Nezu & Nakagawa 1993), mean longitudinal velocity profiles were investigated by fitting the measured profiles to a logarithmic profile. The profile origin was taken at the level where the recorded velocity was zero. All profiles showed a roughness layer right above the rough bed which was between 0.8 and 1.2 D_{50} thick. In this layer, individual roughness elements determine the local flow structure and the flow may become 3D. This layer was therefore omitted from the fitting. It was found that during the unsteady flow, all mean velocity profiles followed a logarithmic law in the inner layer, confirming observations in the literature. However, differences in the profile form were observed. Mean velocity profiles over the logarithmic part of the profile of accelerating and decelerating unsteady flow for the same mean velocity u = 0.2 m/s are shown in Figure 3 where the accelerating flow profile is much steeper than the decelerating one.

The mean velocity development during the two unsteady flow ranges is given in Figure 4. Initially, mean velocity in the accelerating range increases steeply, then more slowly. The decrease in the decelerating range is smoother. A similar behavior is seen for the friction velocity which was determined using the logarithmic mean velocity profile method for all time slices (Figure 5). The peak of the friction velocity is attained before the maximum of the water level (Figure 2) as found by Nezu et al. (1997). Again, friction velocity changes differently in the accelerating and decelerating flow ranges. The mean velocities come to the same value at the peak flow end of the unsteady flow ranges (Figure 4), but the friction velocity u_* does not (Figure 6). The different dynamics of mean velocity and friction velocity during the unsteady range for accelerating and decelerating flow are also evident when the bed shear velocity is plotted against the corresponding mean velocity (Figure 5). It decreased linearly in the decelerating flow range, but shows a more complex relationship in the accelerating flow. For comparable mean velocities in the two unsteady flow ranges, friction velocities are different. This difference confirms the different velocity profile slopes seen in the logarithmic layer (Figure 3).

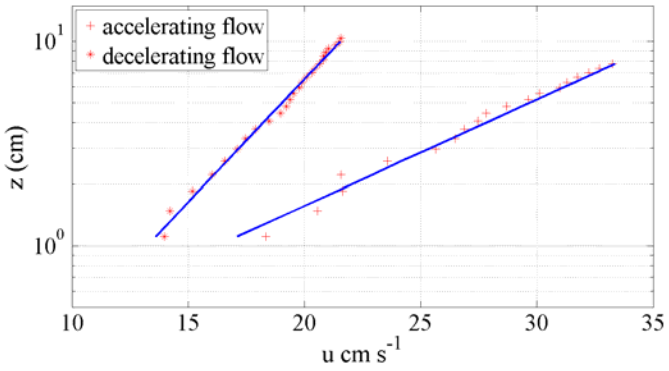

Figure 3. Examples of mean longitudinal velocity profiles for u = 0.2 m/s; solid line: logarithmic profile approximation

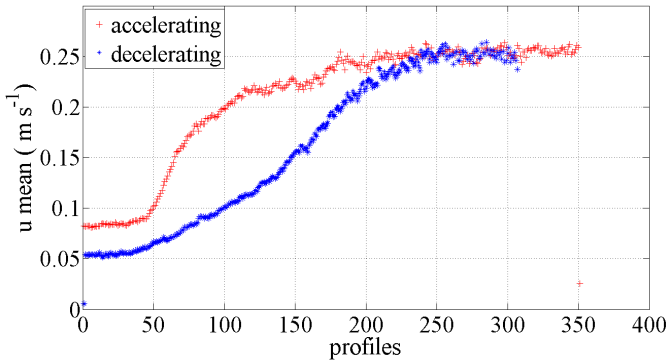

Figure 4. Mean longitudinal velocity distribution for the unsteady range

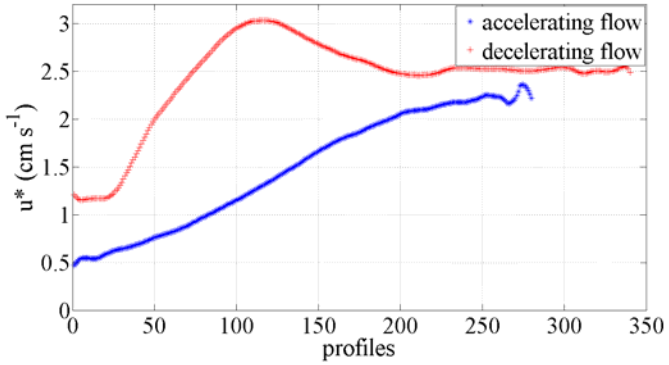

Figure 5. Friction velocity u* distribution for the unsteady range

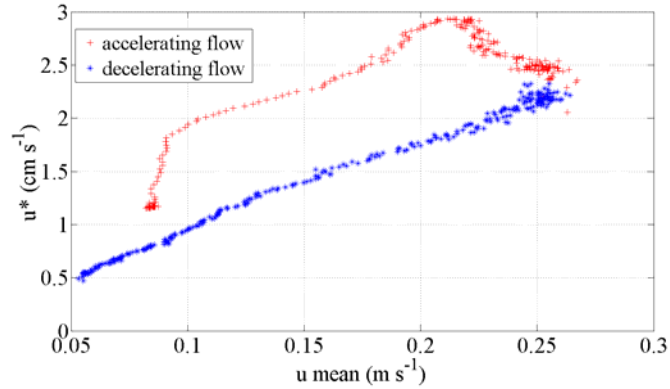

Figure 6. Mean longitudinal velocity and shear velocity development during the unsteady range of the hydrograph

3.2 *Sediment resuspension*

The quasi-instantaneous backscattering intensity profiles recorded by the ADVP are a measure for the concentration of sediment particles in the water column. In low sediment concentration flows, acoustic methods may have difficulty determining the sediment particle concentration correctly, due to the relatively low number of particles inside the acoustic beam. Therefore, in this study, backscattering intensity was not converted into sediment concentration. Instead, backscattering intensity was directly used as an indicator for fine particle resuspension and transport. For the present analysis, the same hydrograph was repeated six times and the data from the six experiments were superimposed for all time slices in order to generate an average data set. Note that during this set of experiments no other flow tracers were in the water. Therefore, the data represent only sediment resuspension dynamics. Results covering the accelerating range, the steady peak flow and the decelerating range are presented in Figure 7 for the particle velocity profiles and in Figure 8 for the backscattering intensity profiles. No data were obtained with the ADVP during the initial base flow, because no particles were suspended and therefore no flow tracers were in the water.

Figure 7 shows a rapid velocity increase near the bottom all along this section of the hydrograph. The particle velocity remains nearly constant during the three ranges of the hydrograph even though the mean flow velocity changes (Figure 4). In the upper part of the water column, particle velocity rapidly falls to zero. Backscattering is initially low, because no sediment is suspended (Figure 8). During the accelerating phase, backscattering intensity rises and remains nearly constant for most of the hydrograph in a layer near the bottom. In the later part, during the decelerating flow, backscattering intensity strongly increases in time and covers a wider range of the water depth, indicating the progressive resuspension of fine particles. Individual peaks in backscattering intensity in Figure 8 document a strong temporal and spatial variability and an event structure of particle suspension process.

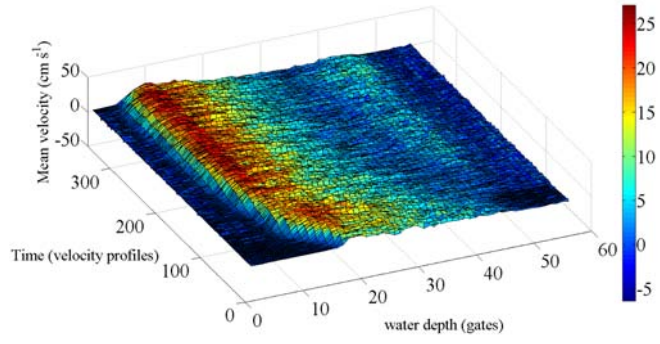

Figure 7. Mean velocities during the unsteady flow range

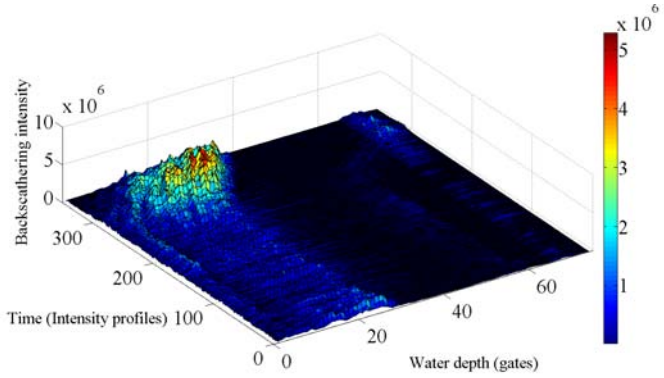

Figure 8. Backscattering intensity during the unsteady flowrange

Some individual profiles for velocity and backscattering intensity, covering the whole range of this part of the hydrograph, were extracted from the above figures and are shown in Figure 9 for particle velocity and in Figure 10 for the corresponding backscattering intensity, in order to present the suspension dynamics during the accelerating, peak flow and decelerating ranges of the hydrograph. The form of all velocity profiles is similar (Figure 9) with a strong velocity gradient near the bed. The maxima of the profiles are found at around 0.25 *h*. Velocities then rapidly decrease and fall to zero at about 0.6 *h*. This indicates that no sediment transport is detected by the ADVP about this level. Sediment particle velocities are similar, even though the flow velocities change during this part of the hydrograph (Figure 4). The corresponding backscattering intensity profiles are plotted in Figure 10. In the accelerating flow range, sediment transport is concentrated in the near bottom layer. In time, backscattering intensity progressively increases in layers further away from the bed. During decelerating flow, backscattering intensity greatly increases in the central layers of the water column, mainly due to the ripples which are formed on the bed and which influence sediment suspension as will be discussed below.

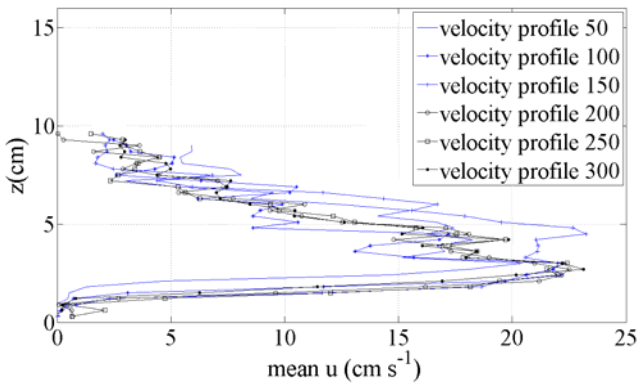

Figure 9. Mean velocity profiles during unsteady flow

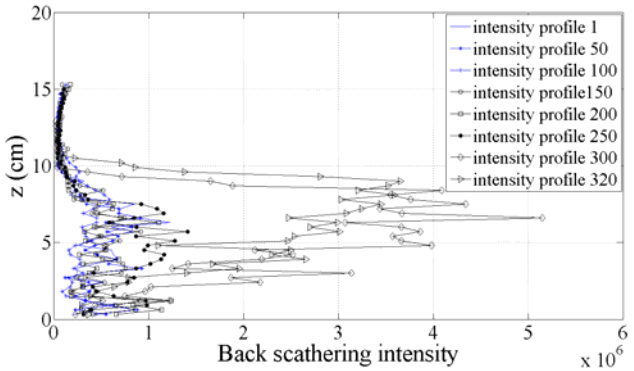

Figure 10. Backscattering intensity profiles during unsteady flow

3.3 *Video imaging*

In low sediment concentration flows which typically occur during the beginning of accelerating flow, acoustic methods may have difficulty determining the sediment particle concentration correctly, due to the relatively low number of particles inside the acoustic beam. Therefore, in this study, video images were recorded in parallel with the ADVP measurements in order to visualize the sediment suspension process during the hydrograph and thereby confirm the above ADVP measurements. Previously (Bagherimiyab et al. 2009), we had shown from video images that sediment transport is initially limited to saltating particles in the near bottom layer in accelerating flow. In the later phase of the accelerating flow and during peak flow, sediment transport near the bed increased and particles were also carried higher into the water column.

In Figure 11, four consecutive images which were taken at a 15 Hz frame rate during the steady peak flow are presented. These images show the passage of one coherent structure reaching up into the water column to about 0.4 *h*, which is then followed by a second one appearing in Figures 11c and d. As seen in Figure 11, suspension is nearly uniform in a shallow layer above the bed (about 2 cm high) and suspension into the water column above occurs in burst-like events. This vertical particle distribution corresponds to the backscattering profiles in Figure 10 where the maximum of the backscatter is near the bottom and significant backscatter is limited roughly to the lower half of the water column. In this flow, turbulence intensity and the strength of the burst events are not sufficient to suspend these particles over the full water depth. Particle transport remained strong in the near bottom layer, in agreement with the ADVP observations shown in Figure 7. Variability in time and space seen in backscattering intensity in Figure 8 can be explained by the burst structure of sediment resuspension observed from the video images.

During this time of the hydrograph, ripples formed rapidly on the bed. The ripples influenced the sediment suspension dynamics (Figures 11 and 12). These bed forms grew within a few seconds with a length of about 0.8 water depth and a height of about 5 to 10 mm (Figure 12). Sediment particles rolled up the ramp of the ripple and were ejected into the water column by vortex shedding from the ripple crest. They then propagated in the flow in the form of a burst as seen in Figure 11. Ripples remained in place when the flow was decelerated down to base flow. Thus, ripples control sediment resuspension into the water column over an extended period of the hydrograph. This is evident from Figures 8 and 10 where backscattering intensity increases towards the end, even though the flow is decelerating.

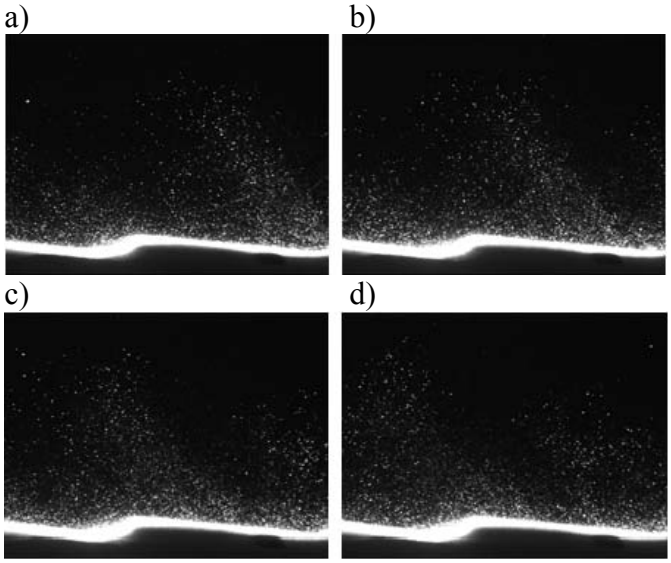

Figure 11. Consecutive images of the video recording (15 Hz frame rate) during the initial peak flow of the hydrograph. Image height is about 9 cm

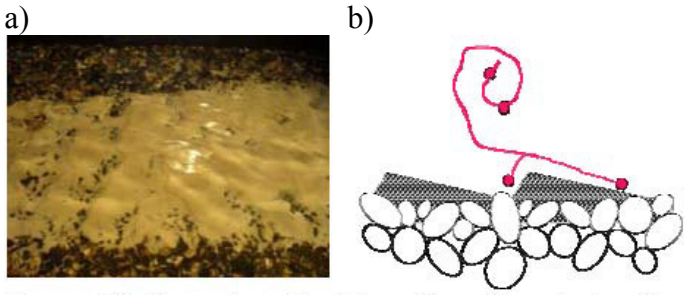

Figure 12. a) Example of bedform formation during the final phase of the unsteady flow range. b) Schematics of the observed sediment transport shown in Figure 11

4 CONCLUSION

Accelerating and decelerating flow over a rough bottom was investigated in a laboratory open channel. Even though the discharge was changed linearly at the same rate in both unsteady flow ranges, the change of relative submergence was not linear and it was different in the two flow ranges, resulting in considerable differences in the flow dynamics. During the accelerating range, both mean velocity and friction velocity initially increased strongly and less thereafter. Two ranges with significantly different slopes were observed during accelerating flow when bed shear velocity was plotted against mean velocity. This indicates that an internal flow adjustment takes place. This adjustment may affect the turbulence structure which is responsible for fine sediment particle resuspension in channels and rivers. During decelerating flow, only one slope and thus one relationship between bed shear velocity and mean flow velocity was found throughout the unsteady flow range. Furthermore, systematically higher friction velocities were observed in accelerating flow than in decelerating flow for comparable mean flow velocities. This indicates that the same change of relative submergence generates different flow dynamics during the accelerating and decelerating flow ranges.

The investigation of unsteady open-channel flow over a coarse bed with a fine sediment layer was limited to the observation of dynamics in velocities and backscattering intensity produced by suspended sediment particles serving as a tracer. It shows that acoustic techniques can be successfully applied to backscatter intensity profiles with high spatial and temporal resolution in unsteady flow. No fine particle transport occurred during the initial phase of the unsteady flow, and particle resuspension was progressively intensified during the unsteady flow range. Even though the concentration of suspended particles was too low to invert the backscattered intensity signal into particle concentration, the ADVP is sensitive enough to capture clean signals for the time history of sediment suspension. Optical methods which were applied simultaneously helped to verify and to interpret the ADVP data and to visualize the physical processes leading to suspension. The combination of acoustical and optical methods provides for an ideal approach in studying resuspension in unsteady flow. An event structure in resuspension is seen by both methods. When the flow had sufficiently accelerated, fine sediment was resuspended in bursts into the intermediate layers of the water column and at the same time, rapidly created nearly stationary ripples during the final phase of the accelerating flow range. Vortices shedding from the ripple crests produced most of the sediment resuspension in the form of events, making resuspension intermittent. High sediment resuspension continued to occur during the decelerating flow even though the flow velocity decreased. This phenomenon is attributed to the presence of ripples which remained in place dur-

ing this range of the hydrograph. However, during our experiments, sediment particles were not suspended into the upper 40% of the water column. Hydraulic parameters, such as water depth, mean velocity time development and profile form were not affected by the presence of fine sediment particles.

The results of this study have verified existing concepts of unsteady flow. However, new and detailed results made possible by combining the ADVP and imaging techniques provide valuable insight into the dynamics of fine sediment resuspension under unsteady flow conditions which were not previously possible. Further experiments will be carried out to refine the approach outlined in this paper. In particular, using multi-frequency ADVP (Hurther et al. 2007) on simultaneously present flow tracers and sediment will help in understanding the relationship between flow and particle resuspension.

ACKNOWLEDGEMENT

This study is supported by the European Commission (FP6; RII3; Contract no. 022441) HYDRALAB III–SANDS. The technical assistance of C. Perrinjaquet is greatly appreciated.

REFERENCES

Afzalimehr, H., & Anctil, F. 2000. Accelerating shear velocity in gravel-bed channels. J. Hydrol. Sci., 45, 113- 123.

Akhavan, R., Kamm, R. D., & Shapiro, A. H. 1991. An investigation of transition to turbulence in bounded oscillatory Stokes flows. I: Experiments. J. Fluid Mech., 225, 395–422.

Bagherimiyab, F., & Lemmin, U. 2009. Velocity and turbulence distribution in unsteady rough-bed open channel flow. Proceedings of the 33rd IAHR Congress, 9 – 14 August 2009, Vancouver, Canada.

Bagherimiyab, F., Lemmin, U., Hurther, D., & Thorne, P. D. 2009. A study of bottom boundary layer dynamics in unsteady sediment-laden open-channel flow using acoustic profiling. Proceedings of the 33rd IAHR Congress, 9 – 14 August 2009, Vancouver, Canada.

Blanckaert, K., & Lemmin, U. 2006. Means of noise reduction in acoustic turbulence measurements. J. Hydr. Res., 44, 3-17.

Bricault, M. 2006. Rétrodiffusion acoustique par une suspension en milieu turbulent: application à la mesure de profils de concentration pour l'étude de processus hydrosédimentaires.Doctoral Thesis, INP Grenoble, France.

Cellino, M., & Lemmin, U. 2004. Influence of coherent flow structures on the dynamics of suspended sediment transport in open-channel flow. J. Hydr. Eng., 130, 1077-1088.

Franca, M.J., & Lemmin, U. 2006. Eliminating velocity aliasing in acoustic Doppler velocity profiler data. Meas. Sci. Technol., 17, 313-322.

Hayashi, T., Ohashi, M., & Oshima, M. 1988. Unsteadiness and turbulence structure of a flood wave. Proc., 20th Symp. on Turbulence, 154–159 (in Japanese).

Hurther, D., Lemmin, U., & Bricault, M. 2007. Multistatic acoustic Doppler profilers for fine-scale studies of velocity and particle flux processes. Proceedings UAM07, Heraklion, Greece.

Jensen, B. L., & Sumer, B. M. 1989. Turbulent oscillatory boundary layers at high Reynolds numbers. J. Fluid Mech., 206, 265–297.

Lhermitte, R., & Lemmin, U. 1994. Open channel flow and turbulence measurement by high-resolution Doppler sonar. J. Atm. and Ocean. Tech., 11, 1295-1308.

Nezu, I. 2005. Open-channel flow turbulence and its research prospect in the 21st century. J. Hydr. Eng., 131, 229-246.

Nezu, I., & Nakagawa, H. 1993. Turbulence in open channel flows. Balkema, Rotterdam, NL.

Nezu, I., Kadata, A., & Nakagawa, H. 1997. Turbulent structure in unsteady depth-varying open-channel flows. J. Hydr. Eng., 123, 752-763.

Shen, C., & Lemmin, U. 1996. Ultrasonic measurements of suspended sediments: A concentration profiling system with attenuation compensation. Meas. Sci. Tech., 9, 1191-1194.

Shields, A. 1936. Anwendung der Aehnlichkeitsmechanik und der Turbulenzforschung auf die Geschiebebewegung. Mitt. Preuss. Versuchsanstalt für Wasserbau, Heft 26.

Sutter de, R., Verhoeven, R., & Krein, A. 2001. Simulation of sediment transport during flood events: laboratory work and field experiments. Hydrol. Sci., 46, 599-610.

Thorne, P.D., & Hanes, D. M. 2002. A review of acoustic measurement of small-scale sediment processes, Continental Shelf Research, 22, 603–632.